

Magnetic excitations in amorphous $\text{Fe}_{75}\text{P}_{15}\text{C}_{10}$ †

H. A. Mook

Solid State Division, Oak Ridge National Laboratory, Oak Ridge, Tennessee 37830

C. C. Tsuei

IBM Thomas J. Watson Research Center, Yorktown Heights, New York 10598

(Received 21 March 1977)

Neutron scattering techniques have been used to measure the magnetic excitations in the amorphous ferromagnet $\text{Fe}_{75}\text{P}_{15}\text{C}_{10}$. Triple-axis measurements show a distinct spin-wave excitation at small momentum transfers that closely obeys a quadratic dispersion relation $E = DQ^2$ for D equal to about $120 \text{ meV } \text{Å}^2$. Time-of-flight polarized-beam measurements made in the vicinity of the first peak in $S(Q)$ near 3 Å^{-1} show excitations that reach a minimum energy at the maximum in $S(Q)$. These excitations are similar to the roton excitations in ^4He except that they are rather broad in energy since they are able to decay into single-particle states. A contour map is presented which shows the scattering measurements in the neighborhood of 3 Å^{-1} and the results are compared with calculations of magnetic excitations in amorphous systems.

I. INTRODUCTION

In the last few years a number of materials have been discovered that are both amorphous and ferromagnetic. A comprehensive review of these materials may be found in Ref. 1. It is of interest to examine the magnetic excitations in these materials and neutron scattering measurements have been performed for several metallic glasses.²⁻⁷ Most of the measurements have been restricted to very small momentum transfers and have been performed with unpolarized neutron beams. The only measurements made with momentum transfers in the region of the first peak of $S(Q)$ were those on Co_4P discussed in Refs. 2 and 3 and measurements on TbFe_2 given in Ref. 5. The TbFe_2 system is complicated because of the two magnetic atoms and it is hard to interpret the excitation spectrum of this material except at small momentum transfers. The Co_4P measurements showed interesting magnetic excitations in the neighborhood of the first peak in the static structure factor $S(Q)$, and it was suggested that these excitations were analogous to the roton excitations observed in ^4He .

Unfortunately, Co is not an easy material to use for neutron scattering measurements because it has a large incoherent scattering cross section that results in a high background counting rate for the experiment, and it also has a non-negligible absorption cross section for neutrons which adds to the difficulty of the experiment. For this reason only a limited amount of information could be obtained about the magnetic excitations in this material. It was thus decided to perform a series of measurements on an iron-based amorphous ferromagnet. Iron has both a low in-

coherent scattering cross section and low neutron absorption so that more detailed measurements are possible for the $\text{Fe}_{75}\text{P}_{15}\text{C}_{10}$ system. Nevertheless, since sample preparation is difficult, only rather small samples were available for the experiment. Also high incident neutron energies must be used for the experiment so that the incident neutron intensity is reduced considerably over that available from the peak in the reactor Maxwell spectrum that occurs about room temperature. The experiment is thus still difficult and except for small momentum transfers polarized-beam cross-correlation techniques must be used to make the measurements possible.

Two sets of measurements were made on the amorphous $\text{Fe}_{75}\text{P}_{15}\text{C}_{10}$ sample. Triple-axis measurements were made at small momentum transfers where a discrete spin wave with a quadratic dispersion relation was observed. These measurements are similar to those reported by Axe *et al.* in Ref. 4 on a different sample of similar composition. The measurements were very restricted since the spin-wave dispersion relation is such that one cannot conserve both energy and momentum in the scattering experiment; unless the energy transfer is very small or prohibitively high, neutron incident energies are used. The triple-axis measurements thus serve to establish D in the quadratic dispersion relation $E = DQ^2$, but are not useful otherwise. At larger Q , measurements are possible if the spin-wave excitation energy is not too high. Time-of-flight measurements were made near the first peak of the static structure factor $S(Q)$ which occurs at about 3 Å^{-1} . For momentum transfers not near zero polarized-beam measurements are necessary to separate the magnetic scattering from the phonon

scattering since the scattering from the phonons can be much more intense than from the magnetic excitations. Time-of-flight techniques are very useful for amorphous systems since a large number of momentum transfers can be measured simultaneously. Furthermore, cross-correlation techniques can be utilized to improve the signal-to-noise ratio of the experiment.

II. POLARIZED-BEAM TIME-OF-FLIGHT SPECTROMETER

Since the pulsed polarization technique is rather novel, it is worthwhile discussing it in some detail. In this type of experiment the beam intensity is not altered, but the polarization state of the neutron beam is varied as a function of time. In this way all non-magnetic processes are avoided. The feasibility of the technique was demonstrated by Steinsvoll and Virjo,⁸ but to perform experiments of interest the pulsed polarization technique must be combined with the correlation technique.

A schematic diagram of the spectrometer is shown in Fig. 1. A beam of neutrons is extracted from the high-flux isotope reactor and made incident on a ⁵⁷Fe crystal which polarizes the neutron beam. This beam is then made incident upon a sample placed in a strong magnet which aligns all the magnetic moments in the sample along the field. Before the sample there is a rf spin-flip pulser that changes the polarization state of the neutron from along the sample field to opposite the sample field. The cross sections for neutron scattering under these conditions are given by Moon, Riste, and Koehler in Ref. 9. Using their notation, the cross section for a scattering process in which the neutron wave vector changes from \vec{k} to \vec{k}' and its spin state changes from state s to s' while the scattering system goes from state q to q' is given by

$$\frac{d^2\sigma^{ss'}}{d\Omega' dE'} = \sum_q P_q \frac{k'}{k} \left| \langle q' | \sum_i e^{i\vec{k}'\cdot\vec{r}_i} U_i^{ss'} | q \rangle \right|^2 \times \delta \left(\frac{h^2}{2m} (k'^2 - k^2) + E_{q'} - E_q \right), \quad (1)$$

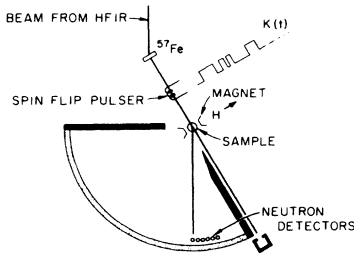


FIG. 1. Schematic diagram of the polarized-beam time-of-flight spectrometer.

where P_q is the probability, the system is in the initial state q , and $U^{ss'}$ is given by

$$U_i^{ss'} = \langle s' | b_i - p_i \bar{S}_i \cdot \bar{\sigma} | s \rangle. \quad (2)$$

b_i is the nuclear coherent scattering amplitude, p is the magnetic amplitude

$$p = (\gamma e^2 / 2mc^2) q S f(K), \quad (3)$$

and \bar{S}_i is defined in terms of the atomic spin operator S by

$$\bar{S}_i = \hat{S} - (\hat{S} \cdot \hat{K}) \hat{K}, \quad (4)$$

where \vec{K} is the scattering vector given by $\vec{K} = \vec{k} - \vec{k}'$.

$\bar{\sigma}$ is the neutron spin operator, γ is the magnitude of the neutron moment in nuclear magnetons, gS is the atomic moment in Bohr magnetons, and $f(\vec{K})$ is the normalized magnetic form factor.

Since in our experiment the applied magnetic field is along the scattering vector $S_{\perp z} = 0$ and all magnetic scattering is spin-flip scattering. In this case then

$$U^{++} = U^{--} = b, \quad U^{\pm} = -p(S_{\perp x} + iS_{\perp y}), \quad (5)$$

$$U^{-+} = -p(S_{\perp x} - iS_{\perp y}),$$

where the neutron is polarized along z . The ground state of the magnetic system is $-NS$ so that the step-up operator associated with the $(+)$ cross section corresponds to magnon creation and neutron energy loss and the step-down operator associated with the $(-)$ cross section involves magnon annihilation and neutron energy gain.

The experiment is then performed in the following manner. Neutrons are brought in to the sample from the ⁵⁷Fe crystal polarized in the $(-)$ state. The spin-flip polarizer is then energized from a computer with a pseudorandom code of pulses of about 10 μ sec duration. During the period of one of these pulses the neutron polarization is reversed to the $(+)$ state so that magnon creation is possible. The neutron is then timed over a $1\frac{1}{2}$ -m flight path and counted in detectors that feed into time scalars in the computer. The pseudorandom code of pulses K is designed so that

$$\frac{1}{N} \sum_i K_i K_{i+j} = \begin{cases} 0, & j \neq 0, \\ 1, & j = 0, \end{cases} \quad (6)$$

where K_i is the i th value of the code and N is the code length. The signal counted by the detectors in the j th time channel is then given by

$$Z_j = c \sum_i \sigma_{i+j}^{ss'} K_i, \quad (7)$$

where σ is the cross section and c is a constant.

Only U^{\pm} contributes when the code element is 1, giving the $(+)$ polarized state, and only U^{-+} contri-

butes when the code element is a -1 , giving $(-)$ polarization. Thus, forming the cross correlation, we obtain the signal T_j in the j th time channel which is given by

$$T_j = \sum_i^N Z_{i+j} K_i = c'(\sigma_j \text{ creation} - \sigma_j \text{ annihilation} + B), \quad (8)$$

where B is a time-independent background, and c' is a constant that depends on the pseudorandom code. In the present experiment we are only interested in magnon creation so we only consider the time channels corresponding to neutron energy loss. These channels give us the time dependence of the cross section and since the flight time over the fixed path length is directly related to the neutron energy, we obtain the cross section $d\sigma^{-+}/dEd\Omega$ immediately from the time-dependent data.

The above technique gives us several distinct advantages in measuring the magnon excitation spectrum. Most important is that the only cross section that results from the measurement is that for spin-flip scattering. All other processes including elastic scattering, phonon scattering, and magnetovibrational scattering cancel in the cross correlation and only contribute to the time-independent background B . Also the duty cycle of the spectrometer is high since the pseudorandom code can contain a $+1$, half the time giving us a 50% on time. Thus the signal-to-noise ratio is very high and very weak excitations can be measured. The counting statistics are calculated from the standard expressions available for the correlation technique and are very favorable in this experiment since there is no elastic peak. The only peak in the spectrum must come from spin-flip scattering. The time-of-flight technique itself is also excellent for amorphous materials since multidetectors make it possible to measure $d\sigma/dEd\Omega$ at a number of momentum transfers simultaneously.

The only disadvantage of the time-of-flight technique is that it is difficult to measure easily at very small scattering angles. Thus very near to $Q=0$, measurements were made on the triple-axis spectrometer. Near $Q=0$, however, the phonon cross section is nearly zero so that measurements are quite straightforward. As one goes away from $Q=0$, polarized beams must be used to get reliable results and the pulsed polarization technique is without competition in this region.

III. SAMPLE

The amorphous alloy $\text{Fe}_{75}\text{P}_{15}\text{C}_{10}$ used in the experiments was obtained by rapid quenching from the liquid state at a cooling rate of around 10^6 K/sec. The details of the alloy preparation and some magnetic properties of this alloy can be found in Ref. 10. The alloy was chosen because of its favorable neutron

scattering characteristics and because it is a relatively well-studied amorphous ferromagnetic alloy system. The alloy contains only one magnetic constituent so that the interpretation of the magnetic excitations in the system is straightforward. The material has low magnetic anisotropy so that its moment can be easily aligned by the 10-kOe field generated by the spectrometer magnet. The Curie temperature of the material is around 600 K so that measurements can be made at room temperature, and its moment of about $1.8\mu_B$ per iron atom is sufficiently high that inelastic scattering measurements are possible. The sample consisted of about 40 foils about 1 in. in diameter and 1.2×10^{-3} in. thick. The static structure factor $S(Q)$ of the sample was measured on a neutron diffractometer and is shown in Fig. 2. The measurements were made with an incident wavelength of 1.15 \AA and with $20'$ collimation before and after the sample. The most noticeable feature of $S(Q)$ is the large peak at 3.05 \AA^{-1} . Our neutron polarized-beam measurements have been concentrated in the vicinity of this peak, and we will see that low-lying magnetic excitations can be observed that have their minimum energies at the maximum value of this peak in $S(Q)$.

IV. RESULTS OF THE INELASTIC SCATTERING MEASUREMENTS

The best way to present results of measurements of magnetic systems is in terms of the generalized susceptibility $\chi(E, Q)$ since this quantity is easiest to compare with theoretical calculations. The generalized susceptibility for spin-flip scattering is given in terms of the cross section by

$$\text{Im}\chi^{-+}(Q, E) = \left[\frac{m_e c^2}{e^2} \right]^2 2 \frac{k_0}{k'} \frac{(q\mu_B)^2 \pi}{N |F(K)|^2} \times \left[\frac{e^{E/KT} - 1}{e^{E/KT}} \right] \frac{d\sigma^{-+}}{d\Omega dE}. \quad (9)$$

The triple-axis data we have obtained are so limited in scope that we have not tried to obtain relative intensities as of function of Q , but to only extract the spin-wave stiffness. In this case then only the raw data will be shown. In all our polarized-beam measurements the data will be presented directly in terms of $\chi^{-+}(Q, E)$. We do not know the form factor $F(Q)$ for our amorphous sample so that the form factor for crystalline iron has been used in converting the measured cross sections to $\chi(Q, E)$.¹¹

Figure 3 shows some of the triple-axis scans. The data presented are the result of subtracting the counts with the sample out of the beam from the counts with the sample in the beam. The scans are constant Q scans and the scattering angle in all cases is very small. The background rate with the sample out shows no structure other than a gradually increasing

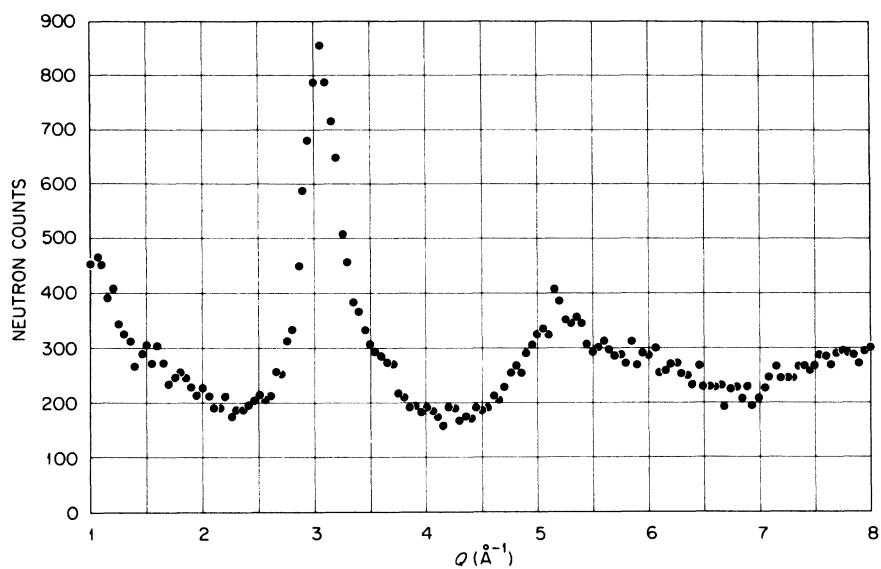


FIG. 2. Static structure factor $S(Q)$ for the $\text{Fe}_{75}\text{P}_{15}\text{C}_{10}$ sample.

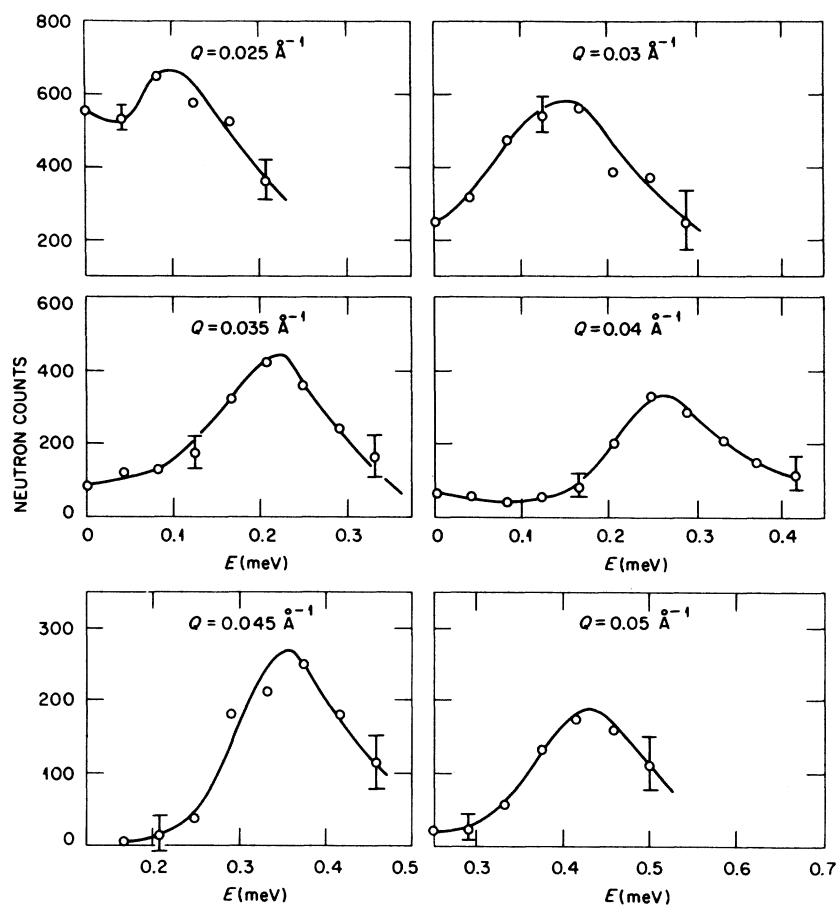


FIG. 3. Spin-wave measurements made at very small momentum transfers using a triple-axis spectrometer.

counting rate as the energy transfer is made higher and the scattering angle is smaller. For instance, for $Q = 0.035 \text{ \AA}^{-1}$, the scattering angle is 0.556° at $\Delta E = 0$ and 0.191° for $\Delta E = 0.33 \text{ mV}$. The error bars are larger at higher energies since the background is higher in this area. The experiment was performed at a fixed outgoing energy of 14.8 meV and a variable incoming energy. 0.10° solar slits were used before and after the sample. The peak widths are consistent with the spectrometer resolution. At a Q much larger than 0.05 \AA^{-1} the spectrometer scattering angle becomes too small to observe a spin wave. This results from the fact that the spin-wave velocity is large compared to the neutron velocity so that it is impossible to conserve both momentum and energy in the scattering experiment. Going to a very high neutron incident energy helps somewhat, but then one needs much better resolution, so that it is difficult to extend the measurements very far out in Q . Axe *et al.*⁴ extended their measurements on a similar sample out to a Q of about 0.18 \AA^{-1} by using incident energies as high as 130 meV . Thus our triple-axis measurements only cover a very restricted range in Q ; however, the measurements are sufficient to give us a value for the spin-wave stiffness constant D . Because the values of Q and E in the experiment are so small, resolution effects are very important and the value of D is greatly affected by spectrometer resolution. While the raw data suggest a D of about 178 meV \AA^2 , the value becomes $120 \pm 25 \text{ meV \AA}^2$ when corrected for spectrometer resolution effects. This value appears to be somewhat below the value of 150 meV \AA^2 reported in Ref. 4. However, the results are essentially in agreement with one another within the experimental errors quoted. Also different samples were used in the two sets of experiments, and while the sample compositions are thought to be very similar, there may be small differences in the samples. For instance, the spin-wave stiffness may be sensitive to small changes in the percentage of iron in the samples or even to the details of the sample preparation.

Most of the polarized-beam measurements were made with an incident neutron energy of 162 meV although a few cross checks of the data were made with lower incident energies. Collimation of $20'$ was used after the monochromator and data were taken simultaneously in 32 separate detectors positioned from 9° to 32° in scattering angle. The detectors are carefully matched in all their characteristics and their neutron capture efficiency is the same within a few percent.

One disadvantage of the time-of-flight technique is that the data collected in one detector are a function of both E and Q so that constant Q scans are not possible. Data from all detectors may be combined and interpolated to achieve constant Q trajectories in reciprocal space; however, we have chosen not to do this and instead have analyzed the data in each detec-

tor separately. Our main interest is to examine the excitations in the neighborhood of the first large peak in $S(Q)$ at 3.05 \AA^{-1} . It turns out that if one uses an incident neutron energy of 162 meV , the time-of-flight scans in the neighborhood of 3 \AA^{-1} are nearly constant Q in nature. For instance, for a scattering angle of 22° , Q only varies from 3.080 \AA^{-1} at an energy transfer $\Delta E = 0$, to 3.180 \AA^{-1} at $\Delta E = 50 \text{ mV}$. Thus the data from each detector can be handled separately with the result that a large number of nearly constant Q scans are available in the Q region near 3.05 \AA^{-1} .

Figure 4 shows a contour map of the $\chi(Q, E)$ measurements centered around 3 \AA^{-1} . Each contour level is $(1/\sqrt{2})^{1/2}$ lower in intensity than the next contour. Not all the contours are closed since they extend out of the range of (E, Q) values collected in the detectors. We notice that $\chi(Q, E)$ peaks up at low energies at the value of Q corresponding to the large peak in $S(Q)$. The structure in $\chi(Q, E)$ is rather broad in energy and Fig. 5 shows the result of a scan near the Q value of 3.05 \AA^{-1} . The Q value of the scan plotted vs the energy transfer ΔE is shown in the top graph. The scan is almost constant Q up to about 50 meV when it starts deviating more rapidly from 3.05 \AA^{-1} . The bottom graph shows $\chi(Q, E)$ plotted vs ΔE . We notice that the maximum in $\chi(Q, E)$ occurs around 19 meV and that the peak is very broad with intensity extending to very low energies. The energy resolution of the spectrometer is sufficiently narrow so that the shape of the peak is not affected much by the spectrometer resolution.

V. DISCUSSION OF RESULTS

In the Co_4P measurements the structure in $\chi(Q, E)$ near the first peak in $S(Q)$ was compared to the roton

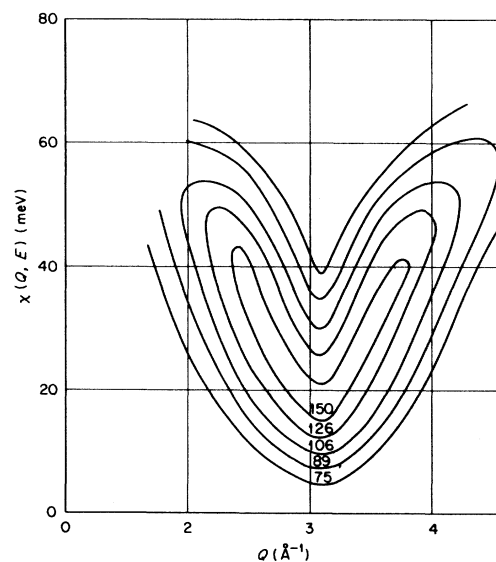


FIG. 4. Contour map of $\chi(Q, E)$ in the neighborhood of the first large peak in $S(Q)$.

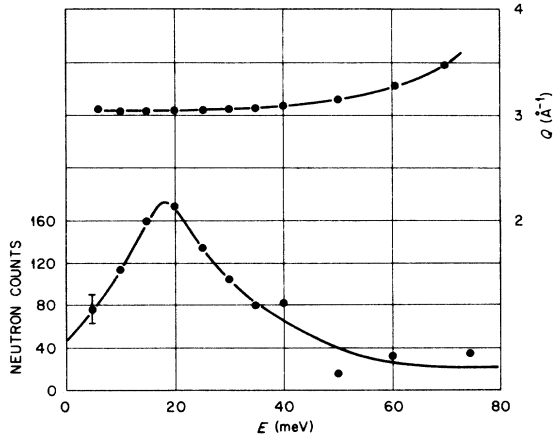


FIG 5. Measurements of $\chi(Q,E)$ obtained in one of the detectors. The top graph shows the Q value of the scan as a function of the energy transfer. Note Q is almost constant over much of the scan.

excitations in ^4He . A graph was shown in which the peaks of $\chi(Q,E)$ nearly fitted on the relation $E = DQ^2$ established from the results near $Q = 0$ if the bottom of the parabola was placed at about 34 meV. Figure 6 shows a similar type of plot for the $\text{Fe}_{75}\text{P}_{15}\text{C}_{10}$ system. Again the relation $E = DQ^2$ shown by the solid line comes close to fitting the experimental data if the bottom of the parabola is placed at 19 meV. There is, however, a noticeable deviation as the energy gets higher, the points lying outside the parabola.

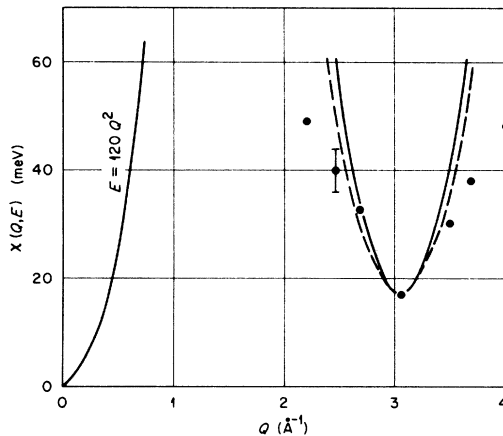


FIG. 6. Curve through the peak positions in $\chi(Q,E)$. Only a small part of the curve around $Q = 0$ has been measured and the solid line shows a continuation of the relation $E = 120Q^2$. The solid line near $Q = 3 \text{ \AA}^{-1}$ shows the relation $E = 120Q^2$ with the bottom of the parabola placed at 3.05 \AA^{-1} and 19.0 meV. The dashed line shows the curve obtained from the theory of Takahashi and Shimizu. The data points are the peak of $\chi(Q,E)$ obtained in scans similar to Fig. 5.

Sum-rule arguments were utilized to show more closely the correlation between the amorphous magnet and liquid ^4He . Again it seems that the excitations in the two systems have a great deal in common. The roton minimum occurs exactly at the peak in $S(Q)$ and there is a gap in both systems at this Q value so that the peak of the excitation spectrum is not at $E = 0$, but at some higher value. However, it is clear in the present data that the excitations are quite broad in energy. It was difficult to establish a width in the Co_4P measurements because constant Q scans were not available. The time-of-flight scans showed rather sharp structure, but widths were difficult to obtain easily since the scans when plotted against Q varied rapidly in E . Sufficient data were not available to construct a contour map of the scattering. The Co_4P dispersion curves were also much steeper in energy than those for the $\text{Fe}_{75}\text{P}_{15}\text{C}_{10}$ so that any broadening in energy at the sides of the parabola would not affect the structure in the scans very much since a large component of these scans was perpendicular to the broadening in energy. A triple-axis constant Q scan through the roton minimum again showed rather sharp structure, but with a tail extending to lower energies. Thus, while the results obtained for the two systems are very similar, it appears that the energy widths of the excitations are larger in the $\text{Fe}_{75}\text{P}_{15}\text{C}_{10}$ system. The increased width in the amorphous Fe-based system may be the result of single-particle excitations extending into the spin-wave region. The position of the single-particle excitations depends on the details of the band structure of the material; however, we might expect that they might lie at higher energies in the Co_4P case since the collective excitations are steeper. From our contour map of $\chi(Q,E)$ for $\text{Fe}_{75}\text{P}_{15}\text{C}_{10}$ we see that the excitations appear to get weaker at higher energies, suggesting that the spin waves may be entering the region of dense single-particle excitations similar to the case for crystalline iron.¹² In this case, the sum rules in Refs. 2 and 3 for $\chi(Q,E)$ are not exhausted by the spin-wave excitations and the analogy between the ^4He system and the magnetic system is not as direct. The difference between the two systems then rests in the fact that the magnons in the amorphous system can decay into single-particle excitations while the phonon excitations near the roton minimum in ^4He have no corresponding states to decay into and thus remain sharp in energy.

Takahashi and Shimizu have developed a theory for the excitations in amorphous magnets near the roton minimum by considering localized magnon states.¹³ The dashed line in Fig. 6 is a fit of their theory to our experimental results. An energy gap of 19 meV was used along with a spin-wave stiffness at $Q = 0$ of 120 meV \AA^2 . The theory seems to give a reasonable fit to the data at the bottom of the parabola, but becomes less good at higher energies.

Calculations of the excitations in amorphous ferromagnets have been performed by Hall and Faulkner¹⁴ and by Alben.¹⁵ The method used by Hall and Faulkner relies on a one-dimensional calculation that can be performed exactly. A tight-binding approximation was used for the Hamiltonian of the electrons in the metal. The model calculation shows structure in $\chi(E, Q)$ similar to that observed, although it is difficult to make an exact comparison with the information that is presently available. It appears that the magnon intensities in the calculation get larger at higher energies, while the measurements show reduced intensities at higher energies. This may be the result of using an approximate Hamiltonian which neglects the effects of the single-particle excitations.

The calculations of Alben are numerical results for spin-wave excitations in a random dense packing model for an amorphous ferromagnet. Again a Heisenberg Hamiltonian is used and the calculations

for $\chi(Q, E)$ look very similar to the measurements on the amorphous system particularly at low energies. The intensities at large energies appear larger than those found in the real amorphous metal, but single-particle excitations have been neglected which would be expected to strongly damp out the magnetic excitations at higher energies. Now that a contour map is available for the measured $\chi(Q, E)$ for an amorphous ferromagnet, it is hoped that more detailed comparisons can be made between the model calculations and the measurements.

ACKNOWLEDGMENTS

The authors would like to acknowledge helpful discussions with D. G. Hall, J. S. Faulkner, and N. Wakabayashi. The spin-flip pulser used in the experiment was built at the Ford Scientific Research Laboratory and made available to us by S. A. Werner.

[†]Research sponsored in part by the ERDA under contract with Union Carbide Corp.

¹G. S. Cargill, III, in *Solid State Physics*, edited by H. Ehrenreich, F. Seitz, and D. Turnbull (Academic, New York, 1975), Vol. 30.

²H. A. Mook, N. Wakabayashi, and D. Pan, *Phys. Rev. Lett.* **34**, 1029 (1975).

³H. A. Mook, D. Pan, J. D. Axe, and L. Passell, *AIP Conf. Proc.* **24**, 112 (1975).

⁴J. D. Axe, L. Passell, and C. C. Tsuei, *AIP Conf. Proc.* **24**, 119 (1975).

⁵J. J. Rhyne, D. L. Price, and H. A. Mook, *AIP Conf. Proc.* **24**, 121 (1975).

⁶J. D. Axe, *AIP Conf. Proc.* **29**, 146 (1976).

⁷J. W. Lynn, G. Shirane, R. J. Birgeneau, and H. S. Chen, *AIP Conf. Proc.* (to be published).

⁸O. Steinsvoll and A. Virjo, in *Neutron Inelastic Scattering*

(IAEA, Vienna, 1968), p. 395.

⁹R. M. Moon, T. Riste, and W. C. Koehler, *Phys. Rev.* **181**, 920 (1969).

¹⁰C. C. Tsuei and H. Lilienthal, *Phys. Rev. B* **13**, 4899 (1976).

¹¹C. G. Shull and Y. Yamada, *J. Phys. Soc. Jpn.* **17**, B111, 1 (1962).

¹²H. A. Mook and R. M. Nicklow, *Phys. Rev. B* **7**, 336 (1973).

¹³Y. Takahashi and M. Shimizu, *Phys. Lett. A* **58**, 419 (1976).

¹⁴D. G. Hall and J. S. Faulkner, in *Proceedings of the Conference on Neutron Scattering*, edited by R. M. Moon, Natl. Tech. Info. Serv. (U. S. Department of Commerce, Springfield, Va., 1976), Vol. II.

¹⁵R. Alben, *AIP Conf. Proc.* **29**, 136 (1976).